

Kinetic plasma microinstabilities

- Gentle beam instability
- Ion- and electron-acoustic instability
- Current-driven cyclotron instability
- Loss-cone instabilities
- Anisotropy-driven waves
- Ion beam instabilities
- Cyclotron maser instability
- Drift-wave instability

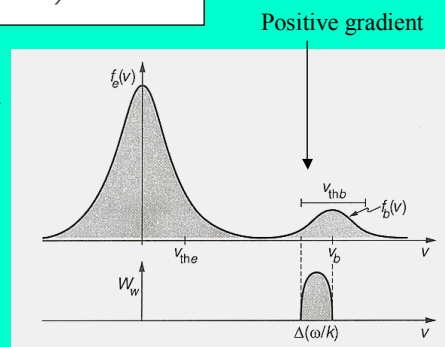
Gentle beam instability I

Electromagnetic waves can penetrate a plasma from outside, whereas electrostatic waves must be excited internally. The simplest kinetic instability is that of an electron beam propagating on a uniform background: *gentle beam* or *bump-on-tail* configuration:

$$\omega_l = \pm \omega_{pe} \left(1 + \frac{3}{2} k^2 \lambda_D^2 \right) + i \gamma_l(k)$$

Few fast electrons at speed $v_b \gg v_{th0}$, but with $n_b \ll n_0$, can excite Langmuir waves.

$$\gamma_l = \omega_l \frac{\pi \omega_{pe}^2}{2 n_0 k^2} \frac{\partial f_{0e}(v)}{\partial v} \Big|_{v=\omega/k}$$



Gentle beam instability II

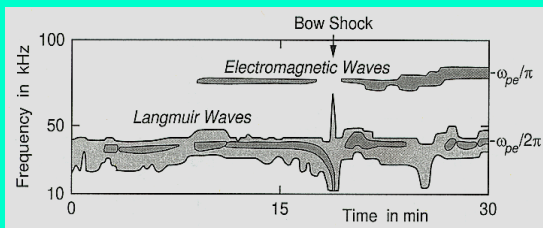
To calculate the growth rate (left as an exercise) of the *gentle beam* instability, we consider the sum of two Maxwellians:

$$f_{0e}(v) = f_0(v) + f_b(v - v_b)$$

The maximum growth rate is obtained for a cool, fast and dense beam.

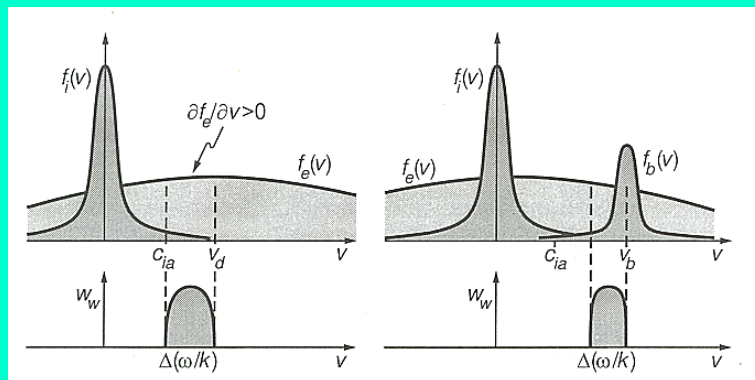
The condition for growth of Langmuir waves is that the beam velocity exceeds a threshold, $v_b > \sqrt{3} v_{th0}$, in order to overcome the Landau damping of the main part of the VDF. Electron beams occur in front of the *bow shock* and often in the solar corona during solar *flares*.

$$\gamma_{gb,max} = \left(\frac{\pi}{2e}\right)^{1/2} \frac{n_b}{n_0} \left(\frac{v_b}{v_{thb}}\right)^2 \omega_l$$



Ion-acoustic instability I

Ion acoustic waves (electrostatic and associated with charge density fluctuations) can in principle be excited by *electron currents* or *ion beams* flowing across a plasma. Two unstable model VDFs are shown below.



The combined equilibrium distribution must have a positive slope at ω/k .

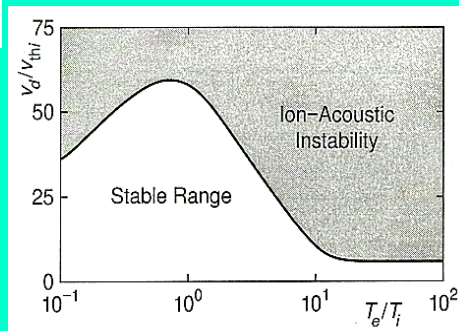
Ion-acoustic instability II

To calculate the growth rate of the *current-driven* electrostatic ion acoustic instability, we consider again the sum of two drifting Maxwellians. Using the ion-acoustic dispersion relation yields the growth rate:

$$\gamma_{ia} = \left(\frac{\pi}{8}\right)^{1/2} \frac{\omega_{ia}}{(1 + k^2 \lambda_D^2)^{3/2}} \left[\left(\frac{m_e}{m_i}\right)^{1/2} \left(\frac{kv_d}{\omega_{ia}} - 1\right) - \left(\frac{T_e}{T_i}\right)^{3/2} \exp\left(-\frac{T_e}{T_i(1 + k^2 \lambda_D^2)}\right) \right]$$

Instability requirements at long-wavelengths:

- small ion Landau damping, $T_e \gg T_i$
- large enough electron drift, $v_d \gg c_{ia}$

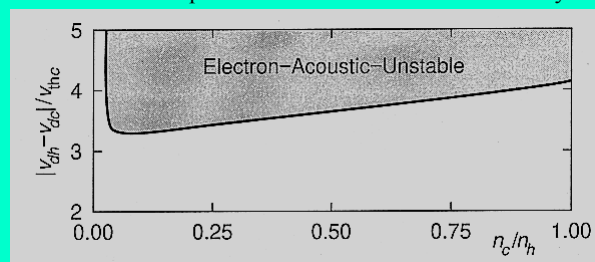


Electron-acoustic instability

Electron acoustic waves (electrostatic and associated with charge density fluctuations) can for example be generated by a two-component (hot and cold) drifting electron VDF, fulfilling the zero current condition: $n_h \mathbf{v}_{dh} + n_c \mathbf{v}_{dc} = \mathbf{0}$. The wave oscillates at the cold electron plasma frequency, $\omega_{ea} \approx \omega_{pc}$. Growth rate:

$$\gamma_{ea} \approx \left(\frac{\pi}{8}\right)^{1/2} \frac{\omega_{pc}}{k^2 \lambda_{Dh}^2} \left(\frac{\mathbf{k} \cdot \mathbf{v}_{dh}}{kv_{thh}} - \frac{\omega_{ea}}{kv_{thh}} \right) \exp \left[-\frac{(\mathbf{k} \cdot \mathbf{v}_{dh} - \omega_{ea})^2}{k^2 v_{thh}^2} \right]$$

Parameter space of the electron-acoustic instability



Current-driven cyclotron instabilities

Ion-cyclotron waves

Parallel current along magnetic field, $\omega \approx l\omega_{gi}$,

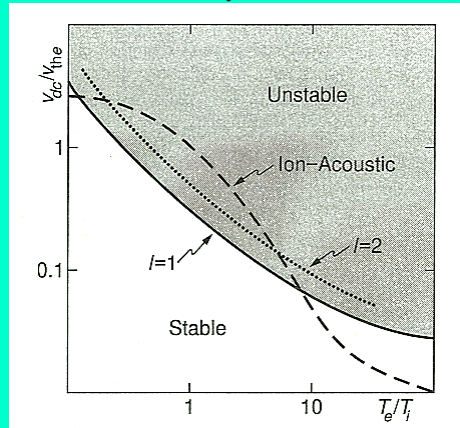
$$k_{\parallel} \ll k_{\perp}, T_i \ll T_e$$

Lower-hybrid modes

Transverse drift current across magnetic field, $\omega \approx \omega_{lh}$,

$$\lambda \ll r_{gi} \text{ ions unmagnetized}$$

Critical current drift speed for the ion-cyclotron wave



Currents can also drive electrostatic ion-cyclotron and lower-hybrid modes.

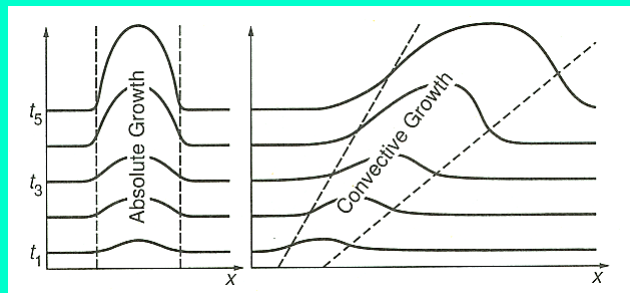
Absolute and convective instabilities

- **Absolute or non-convective instability:**

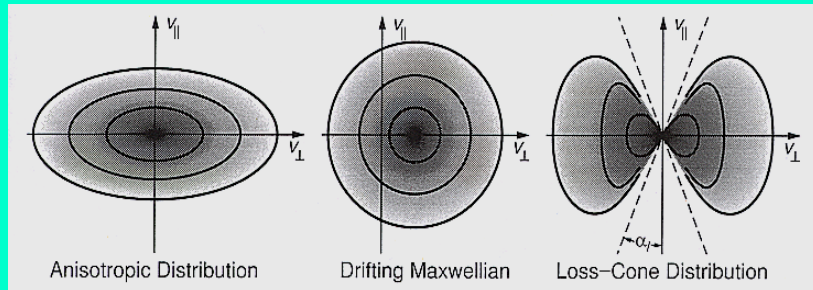
Wave energy stays at the locale of generation and accumulates; amplifies there with time of growth

- **Convective instability:**

Wave energy is transported out of excitation site and disperses; amplifies only over that distance where growth rate is positive



Velocity distributions containing free energy



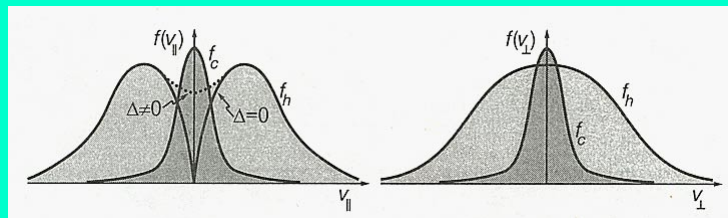
The most common anisotropic VDF in a uniform thermal plasma is the *bi-Maxwellian* distribution. Left figure shows a sketch of it with $T_{\perp} > T_{\parallel}$.

$$f(v_{\perp}, v_{\parallel}) = \frac{n}{T_{\perp} T_{\parallel}^{1/2}} \left(\frac{m}{2\pi k_B} \right)^{3/2} \exp \left(-\frac{mv_{\perp}^2}{2k_B T_{\perp}} - \frac{mv_{\parallel}^2}{2k_B T_{\parallel}} \right)$$

Loss-cone instabilities

Electrostatic electron- and ion-cyclotron waves are very important electrostatic waves, because they occur at principle plasma resonances,

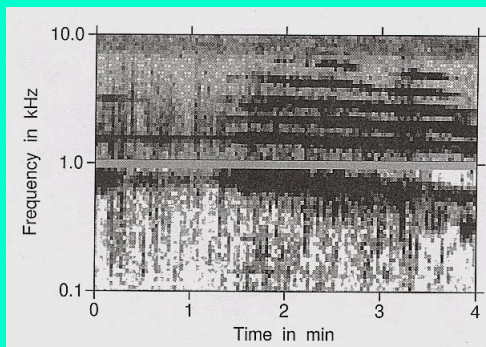
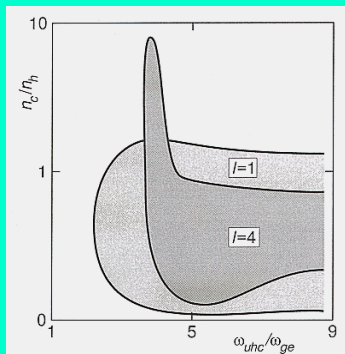
- contribute substantially to wave-particle energy exchange
- are purely of kinetic origin
- require for instability a particular shape of the VDF, with enhanced perpendicular energy, such as thermal anisotropy or a loss-cone



Loss-cone distributions store excess free energy in the gyromotion of the particles and are therefore well suited for exciting waves related to the cyclotron motion.

Electron-cyclotron loss-cone instability

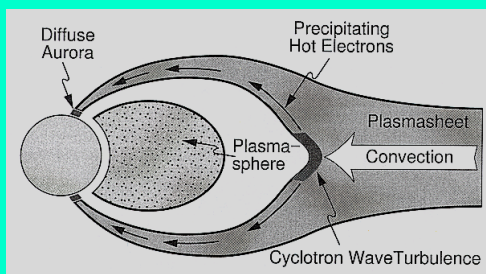
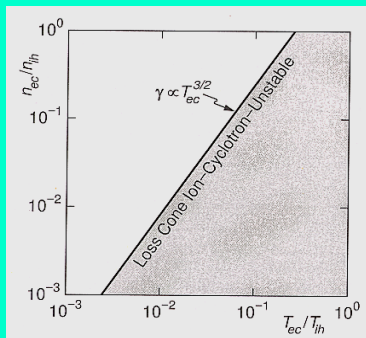
Assume a cool neutralizing ion background (immobile), cold Maxwellian electrons and a *hot dilute loss-cone component* superposed. The dielectric response function is rather complicated (not suggested for an exercise). The region in parameter space of *absolute instability* is illustrated below (left). *Multiple emitted harmonics* of ω_{ge} as observed in the nighttime equatorial magnetosphere are shown on the right.



Electron-cyclotron harmonics are excited by a hot loss-cone distribution.

Ion-cyclotron loss-cone instability

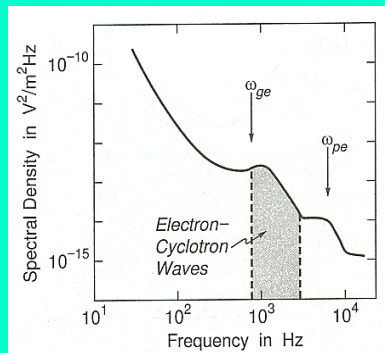
Assume a cold neutralizing electron background and for the ions a cold component with a *hot dilute loss-cone* superposed. The region of instability in parameter space is illustrated below (left). Apparently, the instability depends also on the electron density and temperature. Ring current ions and electrons can due to *cyclotron wave turbulence* scatter into the loss cone and thus precipitate into the polar ionosphere and create aurora (right figure).



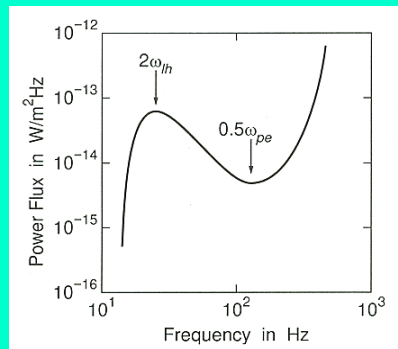
Ion-cyclotron harmonics are excited by a hot loss-cone distribution.

Plasma wave electric field spectra

Plasma sheet electron-cyclotron measured wave spectrum.
Excitation by loss-cone



Auroral hiss, broadband Whistler mode noise; emitted power calculated.
Excitation by field-aligned beam



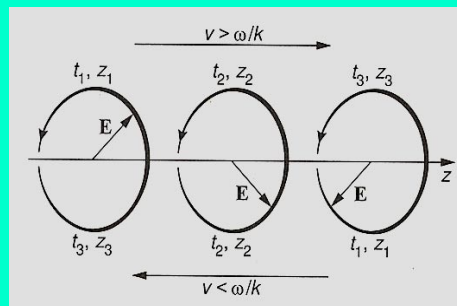
Note that the typical electric field strength is only about $10 \mu\text{V/m}$ and the typical emitted power only a few pW/m^2 .

Cyclotron resonance mechanism

Particles of a particular species with the right parallel velocity will see the wave *electric field* in their frame of reference with the *suitable polarisation* and thus undergo strong interaction with the wave. This is the nature of *cyclotron resonance*, implying that

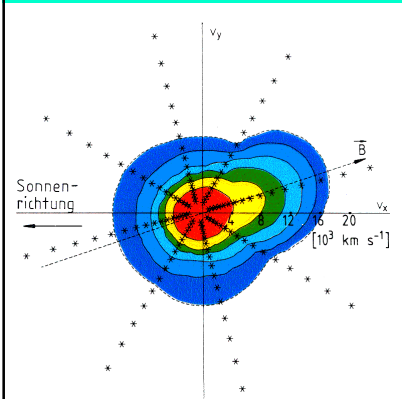
$$k_{\parallel} v_{\parallel} = \omega - l\omega_{gs}$$

The Doppler-shifted wave frequency (as e.g. seen by an ion) equals the l th harmonic of ω_{gi} . **Being for $l = 1$ in perfect resonance, an ion at rest in the wave frame sees the wave at a constant phase.** Otherwise, a slower (faster) ion will see the wave passing to the right (left), and thus sees an L-wave (not) polarised in the sense of its gyration.

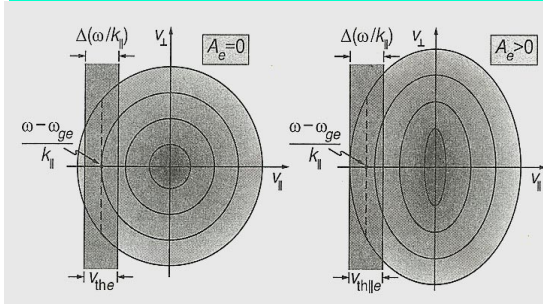


Whistler instability I

The *resonance region* for electrons in the Whistler instability is located in the negative v_{\parallel} plane. An isotropic (left) and anisotropic model VDF with $A_e > 0$ ($A_e = T_{e\perp}/T_{e\parallel} - 1$) is shown. The width of the resonant region is about $v_{th\parallel}$.



Solar wind electrons



Model electron distributions

Whistler instability II

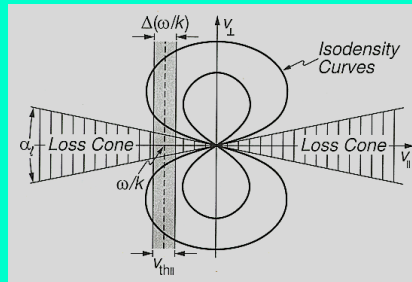
The resonance region for electrons in the *Whistler instability* is located in the negative v_{\parallel} plane, opposite to the wave propagation direction. Consider a dense cold and dilute hot electron components, with $n_h \ll n_c$. Then the growth rate scales like, $\gamma \propto n_h/n_c$. The imaginary part of the dispersion reads:

$$D_i(\omega, k_{\parallel}) = \frac{\sqrt{\pi}\omega}{|k_{\parallel}|v_{th\parallel}} \frac{\omega_{ph}^2}{\omega^2} \left[1 - A_e \left(1 - \frac{\omega_{ge}}{\omega} \right) \right]$$

$$\times \exp \left[-\frac{(\omega - \omega_{ge})^2}{k_{\parallel}^2 v_{th\parallel}^2} \right]$$

Instability requires that

$$\omega < \omega_c = \omega_{ge} A_e / (A_e + 1)$$

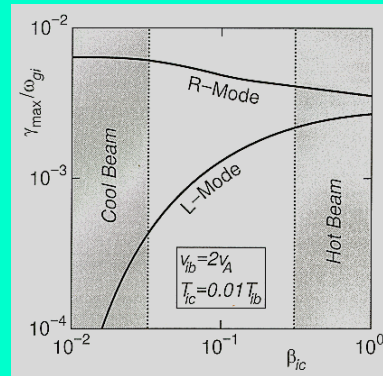
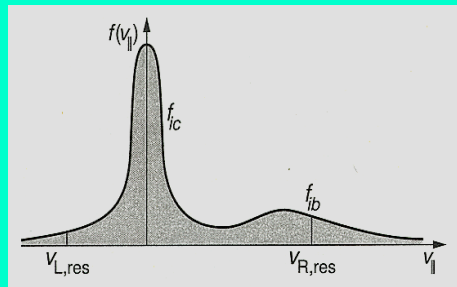


Resonance region and loss-cone VDF

Resonant ion beam instability

Consider an *ion beam* propagating along \mathbf{B} as an energy source for low-frequency electromagnetic waves (see figure below, with a dense core and dilute beam, such that $n_b \ll n_c$). The *resonance speed* for the ions is located in the negative v_{\parallel} -plane for L-waves and positive v_{\parallel} -plane for R-waves and given by:

$$v_{R,L,res} = (\omega \pm \omega_{gi}) / k_{\parallel}$$



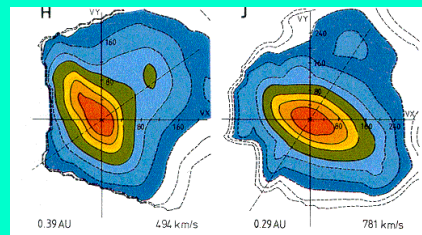
Maximum growth rate for dense core ions and a dilute ion beam

Solar wind proton beam and temperature anisotropy

The most prominent waves below the proton cyclotron frequency, $\omega \ll \omega_{gp}$ are electromagnetic ion cyclotron waves. They can be driven unstable e.g. by *temperature anisotropies*, a free energy source which is most important and frequent in the solar wind (see the right figure).

For parallel propagation the dispersion relation for L and R waves (+ for RHP, and - for LHP) reads:

$$N_{\parallel R,L}^2 = 1 - \frac{\omega_{pe}^2}{\omega(\omega \mp \omega_{ge})} - \frac{\omega_{pi}^2}{\omega(\omega \pm \omega_{gi})}$$



For $k_{\perp} = 0$, the electric field is perpendicular to \mathbf{B} . Ions gyrate in the sense of L-modes, and electrons clockwise in the sense of R-modes.

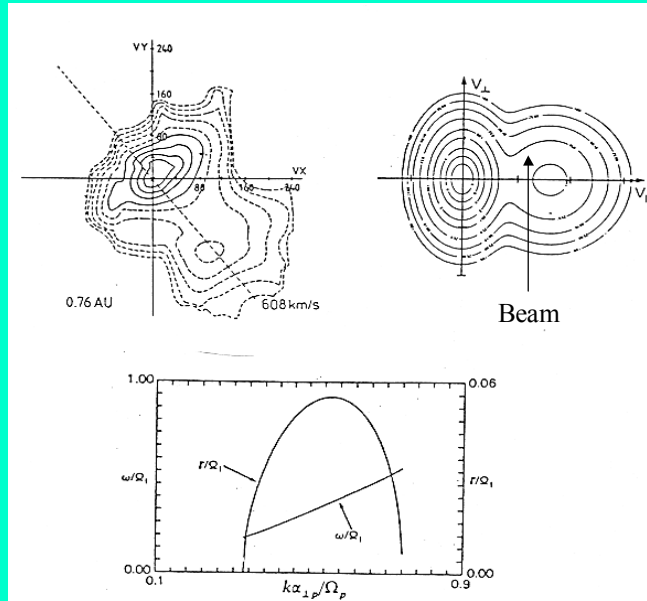
R-wave regulation of solar wind proton beam

- Measured (left) and modeled (right) velocity distribution
- Growth of fast mode R-waves
- **Beam-driven instability**, large beam drift speed, v_b

$$\omega \approx 0.4 \omega_{gp}$$

$$\gamma \approx 0.06 \omega_{gp}$$

Marsch, 1991



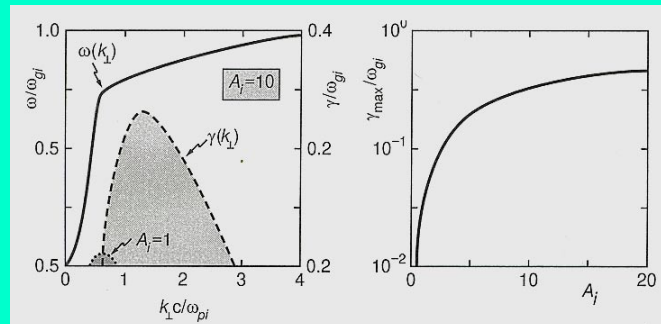
Ion cyclotron instability

The resonance region for ions in the *cyclotron instability* is located in the negative v_{\parallel} plane. A low-frequency instability can occur for $A_i > 0$ ($A_i = T_{\perp i}/T_{\parallel i} - 1$), with the critical frequency given as:

$$\omega < \omega_c = \omega_{gi} A_i / (A_i + 1)$$

At parallel wavelengths shorter than the ion inertial scale, $k_{\parallel}^2 \gg (\omega_{gi}/c)^2$, the **growth rate** (shown below) can be comparatively large:

$$\gamma_{aic} \approx \omega_{gi} \sqrt{\beta_{i\perp} / 2}$$



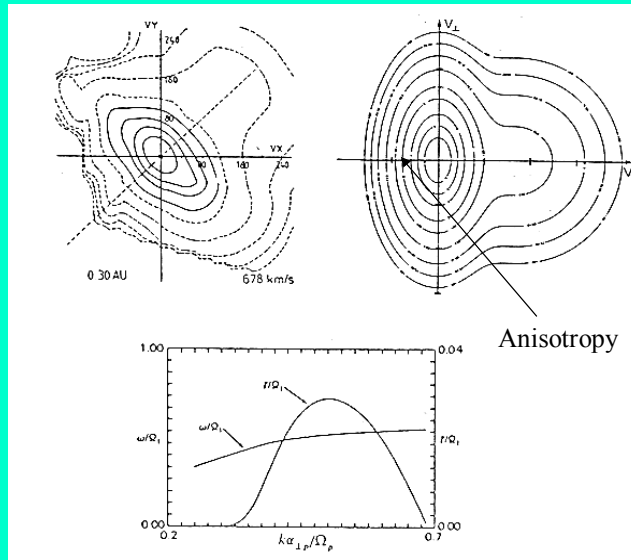
L-wave regulation of solar wind proton anisotropy

- Measured (left) and modeled proton (right) velocity distribution
- Growth of ion-cyclotron L-waves
- Anisotropy-driven instability by large perpendicular T_{\perp}

$$\omega \approx 0.5 \omega_{gp}$$

$$\gamma \approx 0.02 \omega_{gp}$$

Marsch, 1991



Kinetic plasma instabilities in the solar wind

- Observed velocity distributions at *margin of stability*
- Selfconsistent quasi-or non-linear effects not well understood
- *Wave-particle interactions* are the key to understand ion kinetics in corona and solar wind.

Wave mode	Free energy source
Ion acoustic	Ion beams, electron heat flux
Ion cyclotron	Temperature anisotropy
Whistler (Lower Hybrid)	Electron heat flux
Magnetosonic	Ion beams, differential streaming

Marsch, 1991; Gary, Space Science Rev., 56, 373, 1991

Cyclotron maser instability

Gyro- or synchrotron-emission of energetic (>10 keV) or *relativistic electrons* in *planetary radiation belts* can, while being trapped in the form of a loss-cone, lead to *coherent free electromagnetic waves* that can escape their source regions. Direct cyclotron emission fulfils the resonance condition:

$$k_{\parallel}v_{\parallel} - \omega + l\omega_{ge} = 0$$

In the relativistic case the dependence of ω_{ge} on the electron speed must be accounted for: $\omega_{ge} \rightarrow \omega_{ge}/\gamma R$ with the gamma factor:

$$\omega_{ge} \rightarrow \omega_{ge}/\gamma R$$

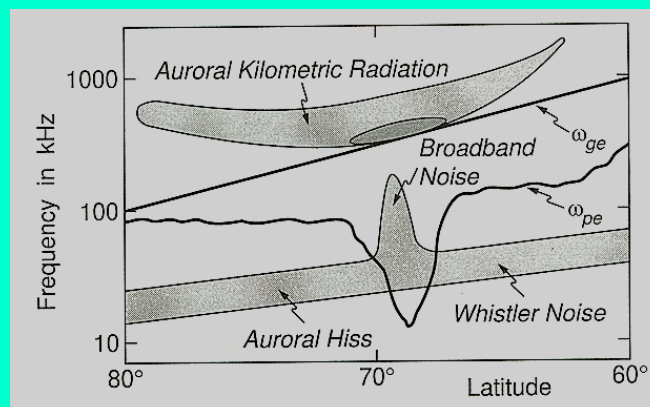
Expansion yields the quadratic equation for the resonance speed, which is an equation of a *shifted circle*,

$$k_{\parallel}v_{\parallel} - \omega + l\omega_{ge} \left[1 - (v_{\parallel}^2 + v_{\perp}^2)/2c^2 \right] = 0$$

along which the *growth rate*, depending on $\partial f(v)/\partial v_{\perp} > 0$, has to be evaluated.

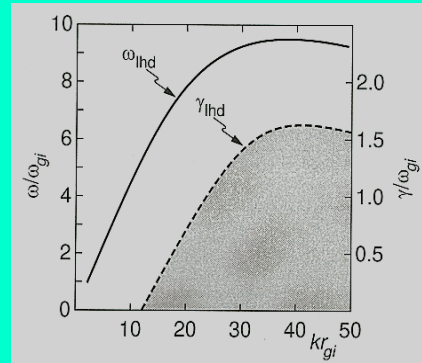
Auroral-zone frequency-latitude spectrogram

For the *cyclotron maser instability* it is important to have a low density and strong magnetic field, like in the *polar cap region* under conditions when aurorae occur, where the ionospheric density is strongly depleted. The types of emissions are sketched below:



Lower-hybrid drift waves

Drift instabilities occur universally in weakly inhomogeneous plasmas. The **lower-hybrid drift** instability is most important, since it is of low frequency and occurs near a natural plasma resonance. **The free energy stems from the diamagnetic drift across a density gradient.** The dispersion relation looks similar to that of the two-stream instability (the ion drift speed is v_{di}):



Lower hybrid drift instability for $r_{gi}/L_n = 0.5$.

$$1 + \frac{\omega_{pe}^2}{\omega_{ge}^2} + \frac{1}{k^2 \lambda_D^2} \frac{\omega_{de}}{(\omega - \mathbf{k} \cdot \mathbf{v}_{di})} + \frac{1}{k^2 \lambda_{Di}^2} = 0$$